Indian Geotech J (October 2022) 52(5):1244–1252
https://doi.org/10.1007/s40098-022-00649-5

ORIGINAL PAPER

Morphological Perspectives to Quantify and Mitigate Liquefaction in Sands

Gali Madhavi Latha[1] · **Balaji Lakkimsetti**[1]

Received: 7 February 2022 / Accepted: 7 July 2022 / Published online: 6 August 2022

Abstract Though the qualitative effects of grain size and grain shape on the tendency or resistance of a sand to liquefaction are well established, quantitative correlations between them are elusive. Most of the studies in this direction used conventional methods to quantify the size and shape of the grains, which include sieve analysis and visual observations. The current study evaluates the size and shape of sand grains through image-based characterizations and relates them to the liquefaction potential of the sand measured in laboratory cyclic simple shear tests. Microscopic images of sand particles were captured and analyzed using MATLAB codes to arrive at the mean particle size, sphericity, roundness, and surface roughness of the sand particles. Cyclic simple shear tests were carried out on sands and sand-like glass beads of different sizes and sands with rounded and angular grains. Results showed that smaller grain size and regular shape of the particle with high sphericity and roundness increase the liquefaction tendency by many folds. In the undrained cyclic simple shear tests carried out in the study, spherical particles liquefied in 8 cycles, whereas river sand with sub-rounded particles liquefied in 13 cycles and manufactured sand with relatively elongated particles liquefied in 16 cycles, particle size being almost same for these three assemblies. Decrease in the liquefaction potential of loose granular assemblies with an increase in grain size and shape irregularity is correlated to the microscopic mechanisms and discussed in light of their tendency for densification, fluid flow patterns and porewater pressure development. Tests with geosynthetic inclusions showed definite reduction in liquefaction potential.

Keywords Liquefaction · Particle shape · Sphericity · Roundness · Cyclic simple shear tests · Geotextile reinforcement

Introduction

Liquefaction can be described as a natural disaster where the ground refuses to support any load and flows like a liquid. Effects of liquefaction can be devastating, causing huge losses to human lives and infrastructure. Many of the recent earthquakes are associated with severe liquefaction events, challenging our preparedness for such calamities. The extreme liquefaction hazards were reported during recent earthquakes of Chile on 27 February 2010 [1], the sequence of 10 earthquakes of Canterbury during 2010–2011 [2], Palu on 28 September 2018 [3] and Durres on 26 November 2019 [4] and witnessed soil liquefaction in sites with grain sizes ranging from coarse silt to fine sand with large variations in the lithology of the deposits. Not much data are available on the shape of grains in these sites. Most of the times, forensic investigations of liquefied sites only talk about the grain sizes and ground motion parameters. The effects of grain shape are usually ignored in liquefaction analysis since grain shape quantifications are not common. Several studies are available on the grain size and shape effects on the mechanical response of sand [5–9]. Most of the studies that investigated the grain shape effects on liquefaction limited the discussion to qualitative shape descriptions, without quantifying the shape of the grains [10–12].

✉ Gali Madhavi Latha
madhavi@iisc.ac.in

[1] Department of Civil Engineering, Indian Institute of Science, Bangalore 560012, India

Liquefaction response of sands can be assessed through laboratory element tests, model tests and field tests. Compared to field tests, laboratory evaluation of liquefaction potential is adopted by several researchers since the tests can be carried out under controlled ground motion conditions that can be accurately simulated in a laboratory setting than in the field. Cyclic triaxial tests, cyclic simple shear tests and cyclic torsion tests are the most widely used element tests and shaking table tests and centrifuge tests with seismic shaker the available model tests for quantifying the liquefaction potential of sands. In laboratory tests, the number of specific cyclic load cycles required to liquefy the soil, cyclic resistance ratio and porewater pressure at liquefaction can be measured. Element tests have additional advantages of controlling sample anisotropy, which plays a major role in the initiation of liquefaction in sands [13]. Among the element tests, cyclic simple shear test can simulate the rotation of principal stresses similar to the field stress conditions during the propagation of shear waves. Unlike the triaxial test and torsion test, direct measurement of shear stresses and shear strains is possible in the cyclic simple shear test. Hence, no correction is needed for the measured cyclic shear stresses for the computation of cyclic stress ratio.

The present study highlights the effects of grain size and shape on the liquefaction potential of sands through image-based shape characterizations and laboratory liquefaction experiments on these sands. Microscopic images of sand particles are analyzed through computational algorithms developed in MATLAB to determine their shape parameters. Cyclic simple shear tests are carried out on sand samples to determine their potential to liquefy under cyclic loading conditions. Shape parameters of sands are correlated to the liquefaction response of sands to bring out the basic mechanisms involved in the particle flow during liquefaction and the effects of microscopic grain size and shape on the macroscopic grain flow during liquefaction. Use of geosynthetics to mitigate liquefaction in sands is explored through a set of cyclic simple shear tests.

Granular Materials Used in Experiments

Two different sands of same grain size with different grain shapes and glass beads of two different sizes are used in the experiments. Samples of sands are scalped from sands of two different origins, to maintain the difference in their grain shape. One of them is a natural river sand with subrounded particles, and the other is a manufactured sand with angular particles. Glass beads are spherical in shape, and they are selected to completely eliminate the shape related effects. Size of glass beads is chosen as 0.7 mm in one set of tests and 1.4 mm in a different set. The difference in the response of spherical glass beads of two different sizes will bring out the effects of grain size on the liquefaction response of granular materials. Comparison of responses of spherical glass beads, subrounded river sand and angular manufactured sand will clearly bring out the effects of particle shape on the liquefaction response. Average size of sand particles determined through sieve analysis is kept as 0.6 mm in all tests. Figure 1 shows the photograph of the granular materials used in this study. Specific gravity (G_s), maximum void ratio (e_{max}), and minimum void ratio (e_{min}) of these materials are determined as per ASTM standard codes D854, D4254 and D4253, respectively. Table 1 presents the grain sizes and physical properties of granular materials.

Shape Characterization of Granular Materials

An advanced digital optical microscope is used for obtaining the microscopic images of representative grains taken from the granular assemblies. While taking the image, the particle orientation is kept in such a way that it is resting on its maximum base [14]. Computation of shape is carried out in three steps—preprocessing, image segmentation and shape analysis. In preprocessing, microscopic images are converted into grayscale images to clearly distinguish the outline of the particle. Image segmentation technique available in MATLAB toolbox is used to convert the grayscale image to a binary image. Geometric computations are carried out on the binary image using special algorithms developed in MATLAB to obtain the shape parameters including Wadell's roundness [15], sphericity [16], and normalized roughness [14, 17, 18]. Table 2 presents the formulae used to compute these parameters.

The shape of a granular particle consists of three scale components—sphericity/form, the macro-scale component, roundness, the meso-scale component and roughness, the micro-scale component. To separate these shape parameters pertaining to different scales, the particle outline from the binary image is expanded in the space domain at an interval of 0.1 radians as a raw profile and is converted to frequency domain using fast Fourier transform (FFT). Since the particle roughness, which is a micro-scale component has high frequency, it can be easily separated from the other two parameters. Comparing the raw and smoothened profiles, the roughness of the particle and the normalized roughness (NR_q) are computed [17, 18]. The computation of sphericity and roundness is then carried out on the smoothened particle profile obtained after removing the roughness component. The meso-scale component roundness represents the roundness of particle corners and the overall shape of the particle. Roundness is computed

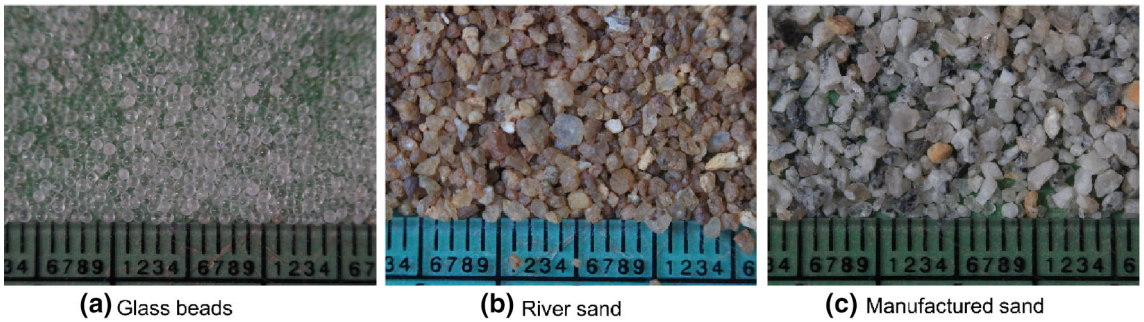

Fig. 1 Photographic images of granular materials used **a** glass beads, **b** river sand, **c** manufactured sand

Table 1 Grain sizes and properties of different granular materials

Granular material	Average grain size (mm)	G_s	e_{max}	e_{min}
Glass beads	0.7	2.52	0.69	0.53
Glass beads	1.4	2.52	0.68	0.52
River sand	0.6	2.62	0.85	0.70
Manufactured sand	0.6	2.66	0.94	0.66

Table 2 Particle shape descriptors and the formulae used to compute them

Descriptor	Formula	Parameter description
Sphericity [15]	$\frac{W}{L}$	W—width of particle L—length of particle
Roundness [16]	$\frac{\sum_{i=1}^{N} r_i/N}{R_{max}}$	r—radius of the circle formed at corners of the projected area of particle N—number of identified corners of the projected area of the particle R_{max}—radius of the largest inscribed circle within the particle
Roughness [17]	$\sqrt{\frac{1}{N}\sum_{i=1}^{N}(y_{ir}-y_{is})^2}$	N—number of measurements y_{ir}—ith coordinate of the raw profile y_{is}—ith coordinate of the smoothened profile
Normalized Roughness [14]	$NR_q = \frac{\text{Roughness}}{L}$	L—length of the particle

from the diameters of the best fit circles for all the corners identified through modified double derivative formula and the diameter of the maximum inscribed circle within the particle boundary, obtained using distance transformation. The macro-scale component sphericity is computed from the largest and smallest dimensions of the particle measured along the major and minor axes of the particle.

Figure 2 shows the microscopic images of representative particles from glass beads, river sand, and manufactured sand.

Figure 3 shows the image analysis of typical particles of glass beads, river sand and manufactured sand with identified corners and best fit circles and maximum inscribed circles within the particle boundaries. These images were taken at 40 × magnification. The roundness, sphericity and normalized roughness values computed for these particles using the equations given in Table 2 are also given in Fig. 3.

In total, 30 particles from each granular material (glass beads, river sand, and manufactured sand) were randomly analyzed using a digital microscope, and the average shape parameters are obtained for the three different granular materials. The average shape parameters for the granular materials are presented in Table 3. Glass beads of both sizes have the same shape parameters.

As observed from Table 3, glass beads are spherical with least roughness value. River sand has higher roundness, higher sphericity and lesser roughness compared to manufactured sand, possibly due to erosion during their transport through water. Particles of manufactured sand are angular and rougher compared to the other two materials because manufactured sand is collected directly from the

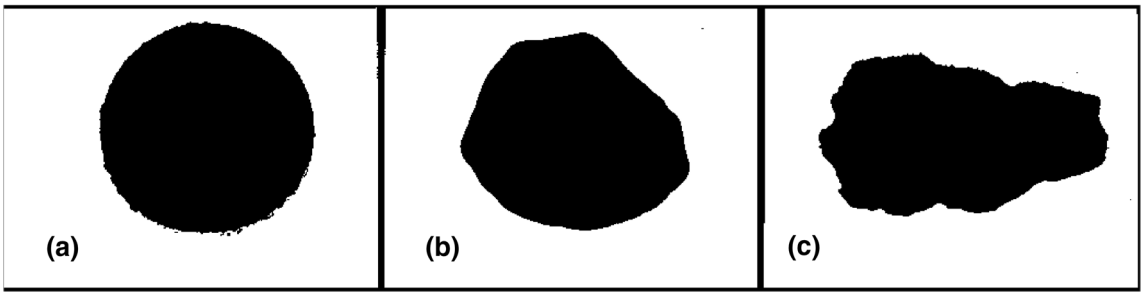

Fig. 2 Microscopic images of typical particles **a** glass beads, **b** river sand, **c** manufactured sand

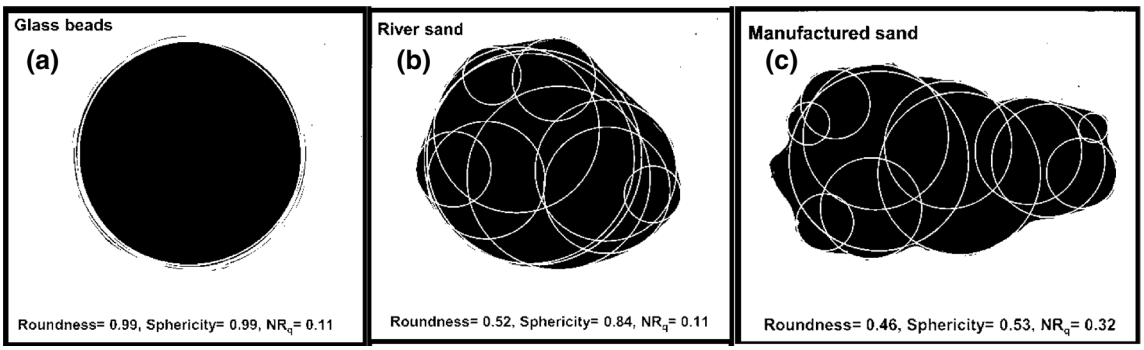

Fig. 3 Image analysis of typical particles **a** glass beads; **b** river sand; **c** manufactured sand

Table 3 Average shape parameters of granular materials

Material	Roundness	Sphericity	Normalized roughness (%)
Glass beads	0.98	0.97	0.11
River sand	0.46	0.86	0.26
Manufactured sand	0.39	0.66	0.34

quarry, where stones are crushed into particles without any polishing. The wide range of roundness (0.39 to 0.98) and sphericity (0.66 to 0.97) used in the experiments is expected to bring out the effects of particle shape on the liquefaction potential clearly from the cyclic simple shear tests.

Cyclic Simple Shear Tests

A cyclic simple shear test setup (GCTS USA make) is used in the present study for carrying out cyclic simple shear tests. The cell of this setup is configured according to the Swedish Geotechnical Institute (SGI) in which a rubber membrane is placed inside the stack of Teflon-coated circular aluminum rings to confine the soil specimen [19]. The setup has a fixed top platen and movable bottom platen. The setup consists of a pneumatic loading system with separate cyclic actuators to apply normal and shear loads and an automatic data acquisition system. Figure 4 shows a photograph of the cyclic simple shear setup with a specimen mounted on it. Figure 5 shows the close-up views of the specimen.

Test specimens of 50 mm diameter and 25 mm height were prepared using dry pluviation. The relative density of sand specimens was kept low at 20%, to facilitate liquefaction in samples. In order to ensure homogeneity of the test specimens, predetermined weight of sample corresponding to the required relative density was poured into the mold from the height of fall corresponding to this density from initial calibration and was mounted on to the cell with minimal disturbances. All specimens are saturated through back pressure, ensuring that cell pressure is always higher than the back pressure, to avoid specimen disturbances. Saturation in the specimens was confirmed through Skempton's parameter B, whose value was maintained about 0.95 in all tests. Specimens were consolidated under an effective isotropic confining pressure of 100 kPa until

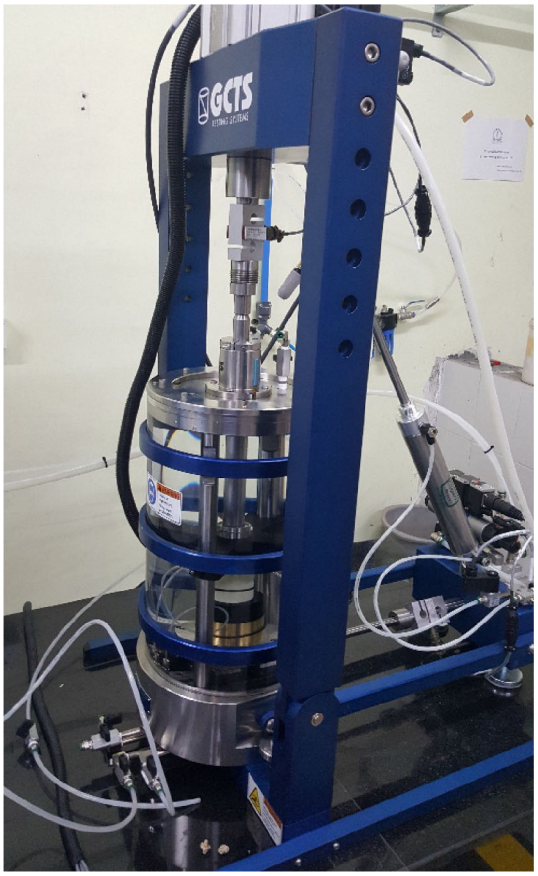

Fig. 4 Cyclic simple shear test setup

volume change in the specimens was ceased. Sinusoidal cyclic load of 1 mm peak-to-peak amplitude and 0.25 Hz frequency was used to shear the specimens under undrained conditions. This corresponds to a shear strain of 2% in the sample. Earthquakes radiate seismic waves in the frequency range of 0.1 to 10 Hz. However, most of the liquefaction-related element tests reported in the literature were conducted in the frequency range of 0.1 to 1 Hz, to ensure adequate time for pore water pressure stabilization inside the specimens [20–22]. Porewater pressure was monitored in the specimen, and the specimen was considered to be completely liquefied when the pore water pressure ratio (r_u) reached a value of 1.0. It must be noted that liquefaction-related particle flow starts in soils along with the buildup of pore water pressure and liquefaction gets initiated before the pore water pressure ratio reaches a value of 1.0. However, several researchers [23–25] have suggested that r_u value reaching 1.0 represents the state of complete liquefaction of sands. As the current study aims at understanding the role of particle morphology on complete liquefaction of sands, the number of cycles needed for reaching the r_u value of 1.0 is compared for sands of different morphologies.

Figure 6 shows the cyclic shear response of glass beads of two different grain sizes, 0.7 mm and 1.4 mm. Under these conditions, the specimen with smaller glass beads liquefied in 8th cycle and the specimen with bigger beads liquefied in the 32nd cycle. These tests clearly indicated that the liquefaction potential of specimens decreases with the increase in the grain size.

The reason for the quicker liquefaction of specimen with smaller grains is explained through Fig. 7. When a specimen is loosely packed, its packing is closer to cubic packing, with void ratio of the specimen closer to the maximum void ratio of the specimen. When loose specimens are sheared, they tend to densify. The densification is manifested as the decrease in volume in a drained test and increase in pore water pressure in an undrained test. If the amount of displacement is needed for smaller grains to get into the densest configuration, which is represented by hexagonal packing being x, larger grains need to displace several times higher displacement than x to reach this state, as shown in Fig. 7.

In the undrained tests carried out in this study, the tendency to densify is manifested through an increase in

Fig. 5 Sand specimen mounted on cyclic simple shear setup

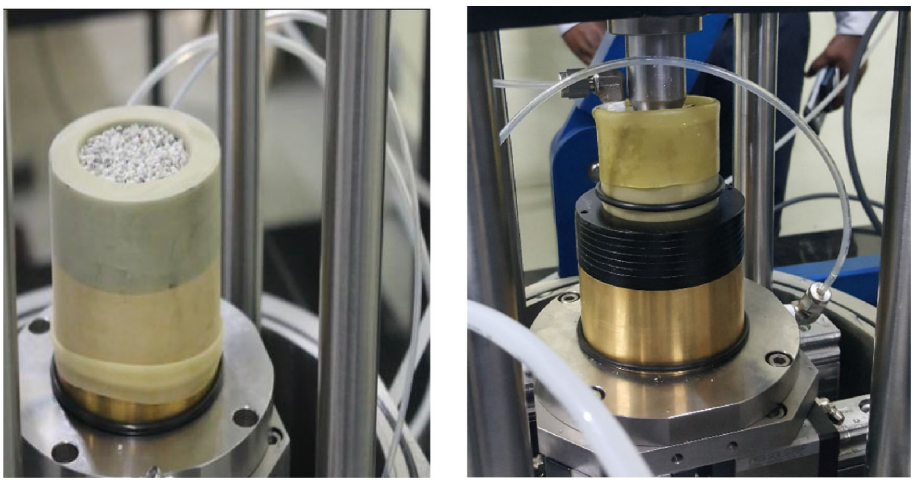

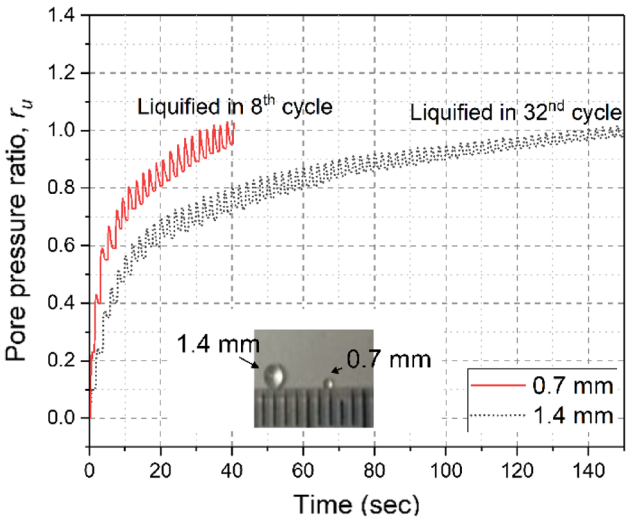

Fig. 6 Effect of size of grain size on the liquefaction potential of granular assemblies

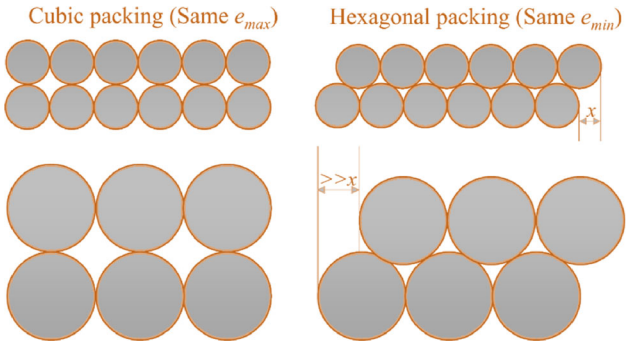

Fig. 7 Grain size effects on densification and liquefaction

porewater pressure. Since the pore sizes in specimens with smaller-sized particles are smaller, the porewater pressure developed in these specimens is high compared to specimens with larger-sized pores, and the porewater pressure increases drastically in these specimens with progressive shearing. Hence, the specimens with smaller-sized particles liquefied quickly compared to the specimens with larger-sized particles.

To study the effects of grain shape, consolidated undrained cyclic simple shear tests were performed on specimens made of the same sized glass beads, river sand, manufactured sand. Response of these three specimens is shown in Fig. 8.

As seen from Fig. 8, glass beads which have regular shape with higher roundness and sphericity liquefied first in the cyclic shear tests. River sand, whose roundness and sphericity fall between glass beads and manufactured sand,

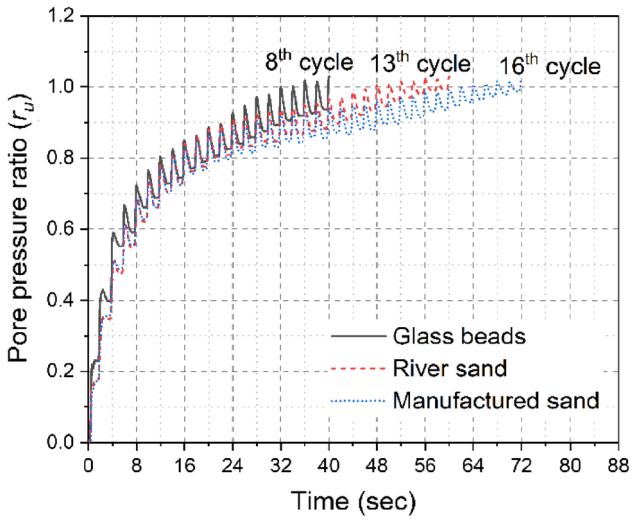

Fig. 8 Effect of size of grain shape on the liquefaction potential of granular assemblies

liquefied next, followed by manufactured sand, whose shape is relatively irregular. Glass beads, river sand and manufactured sand took 8, 13 and 16 cycles, respectively, to reach a porewater pressure ratio of 1.0. These tests clearly highlighted the important effects of grain shape on the liquefaction potential of granular soils. Grain shape effects on liquefaction can be explained through Fig. 9.

As seen in Fig. 9, particles with higher roundness and sphericity roll on each other during shearing. As the shape of the particles becomes irregular, with their overall form deviating much with that of a sphere and their corners becoming more and more sharper, they get interlocked with

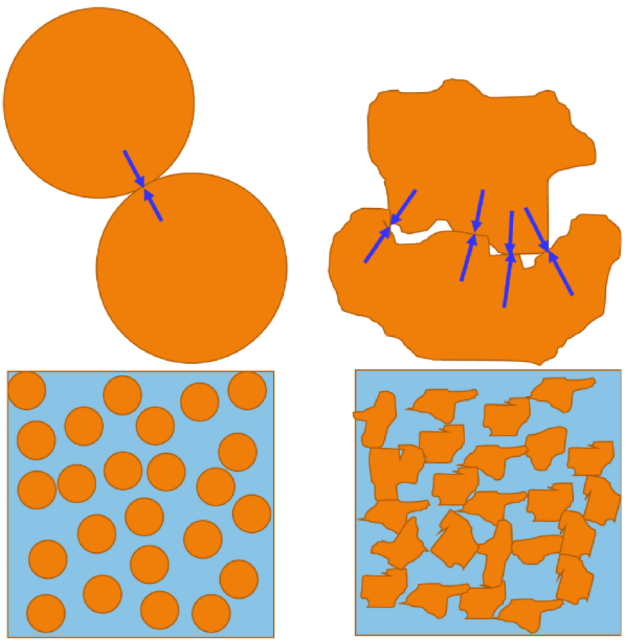

Fig. 9 Grain shape effects on interlocking and liquefaction

each other during shearing. Interlocking provides additional resistance to shear and hence the tendency to get separated from each other to float in the fluid becomes lesser for particles with irregular shape. Manufactured sand specimens took longer time to liquefy because the shear force required to break the interparticle locking is more for the grains because of their relatively irregular shape measured through the lowest sphericity and lowest roundness values (Table 3). Further, tortuosity, which represents the deviation in the fluid path, increases with the irregular shape of the particles. The greater the tortuosity, the lower the water flow through the pore network and lesser the chance for water to separate the particles.

Mitigation of Liquefaction

A set of undrained cyclic simple shear tests were carried out with the three granular assemblies of different particle shapes, with a geotextile layer at the mid-depth of the specimen. Reinforcement layer in the soil prevents the lateral movement of particles because of the lateral interface shear stress developed. With the restricted lateral movement, the particles will not be able to easily get detached from each other to float in the fluid. Geotextile layer also imposes additional confinement on the specimen, demanding higher shear stresses for liquefaction. With this understanding, specimens were prepared with a geotextile layer, as shown in Fig. 10.

The geotextile disk was cut from a roll of non-woven geotextile layer, made of polypropylene yarns. It showed a tensile strength of 7 kN/m in wide width tension test with an elongation of 50% at peak load. Thickness of the geotextile is 1 mm. The geotextile is permeable and allows free passage of water through its pores. Undrained cyclic simple shear tests were carried out using the same input motion parameters as used in unreinforced tests. Results from the tests on geotextile reinforced glass beads, river sand and manufactured sand are presented in Fig. 11.

As seen from Fig. 11, all geotextile reinforced specimens showed higher resistance to liquefaction compared to unreinforced specimens of that specific granular assembly. The specimen of unreinforced glass beads liquefied in 8 cycles, whereas the geotextile reinforced glass beads specimen liquefied in 17 cycles. The beneficial effects of geotextile are more evident in case of sand specimens. The unreinforced river sand specimen liquefied in 13th cycle, whereas the reinforced river sand specimen reached liquefaction in 56 cycles. The unreinforced specimen of manufactured sand reached liquefaction in 16th cycle, whereas the geotextile reinforced manufactured sand specimen got liquefied in 82 cycles. These observations clearly highlight the role of geosynthetics in liquefaction mitigation. Also, higher the surface irregularities of particles, greater are the benefits due to geosynthetic inclusion, because of higher friction developed at the interface. Since the geotextile is deformable, it undergoes successive cycles of compression and expansion during cyclic loading. During successive extensions of the sample, the sheet of compressible non-woven geotextile delays the liquefaction by reducing the interstitial pressure in the sand. When maximum expansion of the inclusion is reached, an interstitial pressure gradient is established in the sample and liquefaction occurs quickly. To visualize this phenomenon, more detailed studies with internal strain monitoring on geotextile surface and measurement of internal pore pressure in the specimens at different locations are needed, which are beyond the scope of the present study.

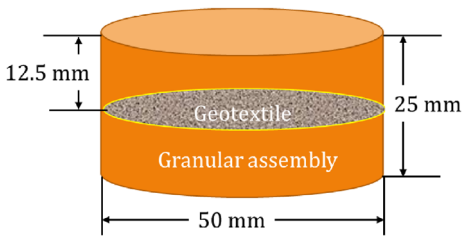

Fig. 10 Schematic diagram of the geotextile reinforced specimen

Among the three granular assemblies tested, glass beads roll and slide on the geotextile, because of their smooth surface and thereby develop less interface friction. Hence, the delay in liquefaction for this case is minimal. Among the sands, manufactured sand particles have maximum surface asperities, and their surface is sharper and less regular compared to river sand. Hence, manufactured sand particles get interlocked in the pores of the geotextile, thereby increasing the interface friction. This is the reason for the maximum delay in liquefaction seen in case of reinforced manufactured sand specimen.

The tensile strength mobilized in the geotextile during the extension cycles of the cyclic loading depends on the interface shear strength between the sand and the geotextile. The shear strength of sand-geosynthetic interface and tensile strength and deformability of geotextile govern the retardation of excess pore water pressure during cyclic loading.

One of the important ideas to translate the current research to field applications is to use particle shape characterization as a tool to quickly assess the liquefaction potential of granular soil deposits in field. Though the current study only talked about the shape analysis of small portions of assemblies, it can be easily extended to real granular assemblies. Further, for constructions where slopes and retaining walls are build using granular materials, choice of fill can be made based on the findings from the present study. In some situations, sand can be

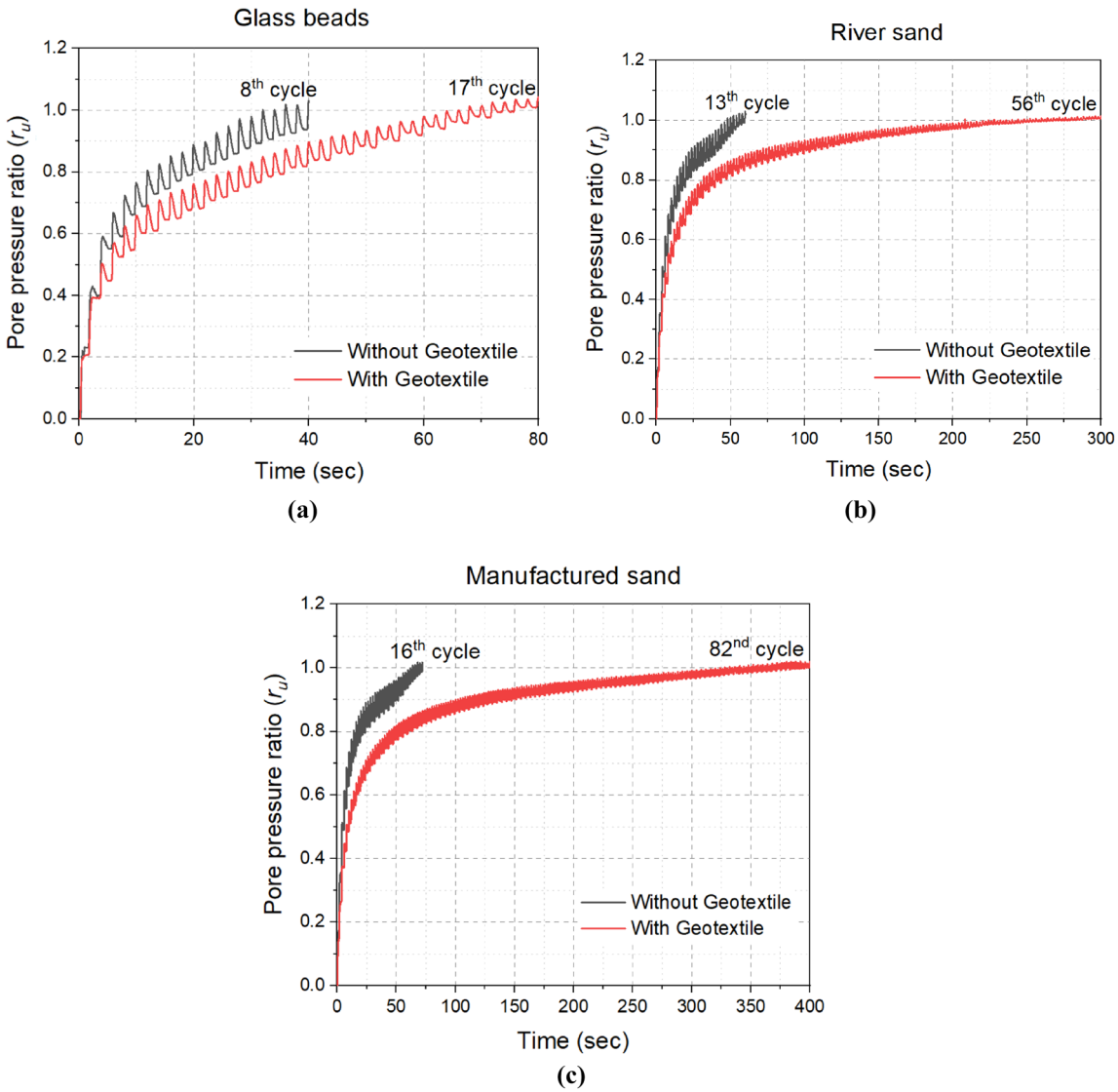

Fig. 11 Response of geotextile reinforced granular assembles under cyclic simple shear **a** glass beads, **b** river sand, **c** manufactured sand

manufactured to specific shapes to avoid the liquefaction-related damages. Reinforcing such granular soil structures with geosynthetics will further reduce the chances of liquefaction, as highlighted from the present study.

Conclusions

The following major conclusions are drawn from the particle shape characterizations and cyclic simple shear tests carried out on granular assemblies.

- Particle size and shape have significant role on the liquefaction resistance of granular assemblies. Among the two sizes of glass beads tested, smaller glass beads liquefied easily because of lesser deformations needed to move toward denser packing, which is manifested in terms of increased pore water pressure through their smaller pores under undrained cyclic loading.
- Particles with higher sphericity of shape and higher roundness of corners easily liquefy under undrained cyclic loading conditions. Among the three different granular assemblies tested, glass beads with maximum sphericity and roundness (close to unity) have liquefied in 8 cycles of sinusoidal cyclic load of 1 mm amplitude and 0.25 Hz frequency. Manufactured sand with least sphericity of 0.66 and roundness of 0.39 has taken 16 cycles to reach liquefaction under the same conditions. River sand with sphericity and roundness between these two assemblies liquefied in 13 cycles. Reasons for the improved liquefaction resistance of manufactured sand are attributed to the particle interlocking, which

increases the shear stress requirement for separating the particles to make them float in water.

- Geosynthetic reinforcement increased the liquefaction resistance of all granular assemblies. Maximum benefit of reinforcement is seen in manufactured sand with relatively irregular shaped particles, because of the increase in interface shear resistance, particle interlocking on the surface of the geotextile and reduced interstitial pore pressure due to the deformability of geotextile.
- Because of their particle shape and associated micro-level interactions, reinforced glass beads, river sand and manufactured sand took about twice, four times and five times as many number of cycles of their unreinforced counterparts for complete liquefaction.
- Results from this study are useful for understanding the effects of particle morphology on soil liquefaction. These results can be directly applied to build geotechnical structures that can withstand liquefaction by using sand manufactured to shapes that are resistant to liquefaction and to design soil reinforcement to further improve the liquefaction resistance of these structures.

Acknowledgements The research presented in this paper is financially supported by the SERB POWER fellowship of the Department of Science and Technology (DST), India. The cyclic simple shear setup used for experiments was procured through the financial support from DST FIST grants. Authors sincerely thank the funding agency for the support.

Funding Funding for this study was provided through Fund for Improvement of S&T Infrastructure (FIST) Phase 3 and SERB POWER FELLOWSHIP (SPF/2021/000041) of the Department of Science and Technology, India and Dam Rehabilitation and Improvement Project (DRIP) of the Ministry of Water Resources (MoWR), Government of India.

Declarations

Conflict of interest The authors do not have any conflict of interest to declare.

References

1. Verdugo R, Gonzalez J (2015) Liquefaction-induced ground damages during the 2010 Chile earthquake. Soil Dyn Earthq Eng 79:280–295
2. Potter SH, Becker JS, Johnston DM, Rossiter KP (2015) An overview of the impacts of the 2010–2011 Canterbury earthquakes. Int J Disast Risk Reduct 14:6–14
3. Jalil A, Fathani TF, Satyarno I, Wilopo W (2021) Liquefaction in Palu: the cause of massive mudflows. Geoenvironment Disast 8:21
4. Mavroulis S, Lekkas E, Carydis P (2021) Liquefaction phenomena induced by the 26 November 2019, mw = 6.4 Durres (Albania) earthquake and liquefaction susceptibility assessment in the affected area. Geosciences 11(5):215
5. Wei LM, Yang J (2014) On the role of grain shape in static liquefaction of sand–fines mixtures. Geotechnique 64(9):740–745
6. Cho GC, Dodds J, Santamarina JC (2006) Particle shape effects on packing density, stiffness, and strength: natural and crushed sands. J Geotech Geoenviron Eng 132(5):591–602
7. Shin H, Santamarina JC (2013) Role of particle angularity on the mechanical behavior of granular mixtures. J Geotech Geoenviron Eng 139(2):353–355
8. Thakur MM, Penumadu D (2021) Influence of friction and particle morphology on triaxial shearing of granular materials. J Geotech Geoenviron Eng 147(11):04021118
9. Yang J, Wei LM (2012) Collapse of loose sand with the addition of fines: the role of particle shape. Geotechnique 62(12):1111–1125
10. Castro G, Poulos SJ (1977) Factors affecting liquefaction and cyclic mobility. J Geotech Eng Div ASCE 103(6):501–516
11. Hird CC, Hassona FAK (1990) Some factors affecting the liquefaction and flow of saturated sands in laboratory tests. Eng Geol 28:149–170
12. Yang J, Dai BB (2011) Is the quasi-steady state a real behaviour? A micromechanical perspective. Geotechnique 61(2):175–183
13. Morimoto T, Aoyagi Y, Koseki J (2019) Effects of induced anisotropy on multiple liquefaction properties of sand with initial static shear. Soils Found 59:1148–1159
14. Vangla P, Roy N, Latha GM (2018) Image based shape characterization of granular materials and its effect on kinematics of particle motion. Granular Matter 20(1):1–19
15. Wadell H (1935) Volume, shape, and roundness of quartz particles. J Geol 43(3):250–280
16. Wadell H (1932) Volume, shape, and roundness of rock particles. J Geol 40(5):443–451
17. Zheng J, Hryciw RD (2015) Traditional soil particle sphericity, roundness and surface roughness by computational geometry. Geotechnique 65(6):494–506
18. Roy N, Vangla P, Frost JD, Latha GM (2021) An enhanced automated particle angularity measurement method. J Test Eval 50(2):20210048
19. Kjellman W (1951) Testing the shear strength of clay in Sweden. Geotechnique 2(3):225–232
20. Hubler JF, Athanasopoulos-Zekkos A, Zekkos D (2017) Monotonic, cyclic, and postcyclic simple shear response of three uniform gravels in constant volume conditions. J Geotech Geoenviron Eng 143(9):04017043
21. Kantesaria N, Sachan A (2021) Cyclic degradation and porewater pressure response of high-plasticity compacted clay. J Geotech Geoenviron Eng 147(11):04021113
22. Kang X, Ge L, Chang KT, Kwok AO (2016) Strain-controlled cyclic simple shear tests on sand with radial strain measurements. J Mater Civ Eng 28(4):04015169
23. Madhusudhan BR, Boominathan A, Banerjee S (2020) Cyclic simple shear response of sand–rubber tire chip mixtures. Int J Geomech 20(9):04020136
24. Rasouli H, Fatahi B (2022) Liquefaction and post-liquefaction resistance of sand reinforced with recycled geofibre. Geotext Geomembr 50(1):69–81
25. Zhang X, Russell AR (2020) Assessing liquefaction resistance of fiber-reinforced sand using a new pore pressure ratio. J Geotech Geoenviron Eng 146(1):04019125